The International Journal of Advanced Manufacturing Technology (2019) 102:17–26
https://doi.org/10.1007/s00170-018-3200-6

ORIGINAL ARTICLE

Research on multi-roll roll forming process of thick plate

Yan Wang[1] · Xinqing Zhu[1] · Qiang Wang[1] · Ximin Cui[1]

Received: 28 June 2018 / Accepted: 12 December 2018 / Published online: 18 December 2018

Abstract
Considering that the non-uniform distribution of the strength in the thick direction will reduce the forming precision during the thick plate bending process, the multi-pass roll forming is an effective process in the production of thick plate. Based on the rebound theory of thick plates, a four-roll roll forming process model was developed. In addition, the multi-pass roll forming control algorithm was established based on the actual roll bending data. The influence of number of rolling bends on the forming quality of the sheet was analyzed qualitatively by numerical simulation. The results indicate that the plastic strain distribution on the surface of the cylinder after the multi-pass roll forming is more uniform, and the rolling bend data multi-pass roll forming control algorithm has strong adaptability, it can not only improve the plate forming quality after multi-pass roll bending, but also can easily realize three-pass roll forming.

Keywords Forming process model · Multi-pass roll forming control algorithm · Numerical simulation

1 Introduction

The multi-pass roll forming process, which is a process method that can effectively improve the forming accuracy of workpieces, has been widely used in the industry. Many theories about multi-pass roll forming have been developed. Milenin et al. [1] proposed the mathematical model of multi-pass rolling and developed the rheological model on the base of the dislocation theory of plastic deformation. Chen et al. [2] investigated the effect of multi-pass rolling upon the mechanical properties of the explosive welding Mg/Al composite plates; the study shows that the explosive welding Mg/Al composite plates have the good surface quality when it was obtained by five passes hot rolling. Gandhi et al. [3] analyzed the formulation of springback and machine setting parameters for continuous multi-pass bending on three-roll bending machines with non-compatible rolls; analytical results of multi-pass cone frustum bending were verified with the cone frustum bending experiments and found to be in good agreement. Luksza et al. [4] found that an increase in the number of passes led to changes in strength and plastic properties; it was confirmed that strength properties grew with increasing number of passes. Hua et al. [5] studied the forming process of multi-pass rolling thin plates based on the elasto-plastic bending theory and established the numerical relationship between the bending moment and the forming curvature; in addition, it was analyzed the effect of the number of roll bending and the thickness of the plate on roll forming quality. Yu et al. [6] have proven that the difference of the initial curvature of each pipe wall segment can be eliminated and unified by multiple times of reciprocating bending, and the residual ovality can be controlled at around 0.35% by the multiple bending processes.

Considering that the multi-pass rolling obtains non-linear features, it is impossible to solve the complicated deformation problem rationally and effectively only by the method of analytic geometry. With the rapid development of computer technology, the finite element simulation provides a better method. Fu et al. [7] proposed an analytical model and ABAQUS finite element model for investigating the three-roll bending forming process, and a reasonably accurate relationship between the downward inner roller displacement and the desired springback radius (unloaded curvature radius) of the bent plate is yielded by both analytical and finite element

✉ Yan Wang
yanwang909909@163.com

[1] Department of Mechanical Engineering, University of Shanghai for Science and Technology, Jungong road 516, Shanghai 200093, People's Republic of China

approaches, which all agree well with experiments. Ktari et al. [8] established a two-dimensional finite element model of three-roll bending machine and deduced the numerical relationship between the roll down and the forming radius of the sheet metal. Shivpuri et al. [9] presents a methodology for roll pass optimization; it uses three-dimensional finite element simulation along with empirical procedures to arrive at an iterative scheme for reducing the number of passes and improving metal flow in the passes; it was proven to be effective in reducing the area and distribution of effective strain in rolled products. Yuan et al. [10] presents a new method for modeling a rod and wire continuous rolling process, and three-dimensional FEM is used to prove the effectiveness of the method. Shin et al. [11] presents an analysis of a seven pass square-to-round sequence using a computationally effective quasi-three-dimensional finite-slab element code; it was verified that the calculated values of exit cross-sectional areas and roll separating forces agree well with experimental values. The current research focuses on the forming quality change with the number of rolling; there is few research on the determination of rolling number, and there are few analyses about how to select the appropriate track to satisfy the plate forming quality.

In this paper, a four-roll bending forming process model was established based on the rebound theory of thick plates. The influence on the forming quality of the plate was analyzed by a two-dimensional dynamic model of four-roll bending. Considering that the four-roll bending forming is affected by many factors, multi-pass roll-bending control algorithm is constructed based on the actual roll bending data, and it has been verified effective through experiments.

2 Four-roll bending process model

2.1 Four-roll bending forming process

Rolling process changes with the thickness of the sheet. Figure 1 shows the roll bending process commonly used in thick plates: (a) alignment, (b) pre-bend, (c) primary rolling, (d) second rolling, (e) third rolling, and (f) end of rolling. In general, primary roll, second roll, and third roll are collectively referred to as continuous rolling.

The specific steps are as follows: Firstly, as shown in Fig. 1a, the left roll is lifted to align the plates. Subsequently, as shown in Fig. 1b, the right roll is lifted to bend the end of the sheet. After pre-bending, the top roll starts and roll the plate firstly, as shown in Fig. 1c. In the second rolling process, as shown in Fig. 1d, the right roll continues to lift and the top roll rotates in reverse. Then, the right roll is lifted again, the top roll rotates in the forward direction, and the plate is transited to the third rolling process, as shown in Fig. 1e. At this point, the roll-formed tube is divided into three sections: pre-bend section, continuous roll bending section, straight edge section, and the forming radius of the continuous roll bending section is the main size of the tube.

2.2 Four-roll bending forming process model

The displacement of the side roll during the first rolling is particularly critical for large thick plate. Under normal circumstances, the displacement of the first side roll is not greater than 1/2 of the maximum displacement. With the experience increased, the displacement of the secondary trial will gradually increase. Increasing the displacement of the first rolling

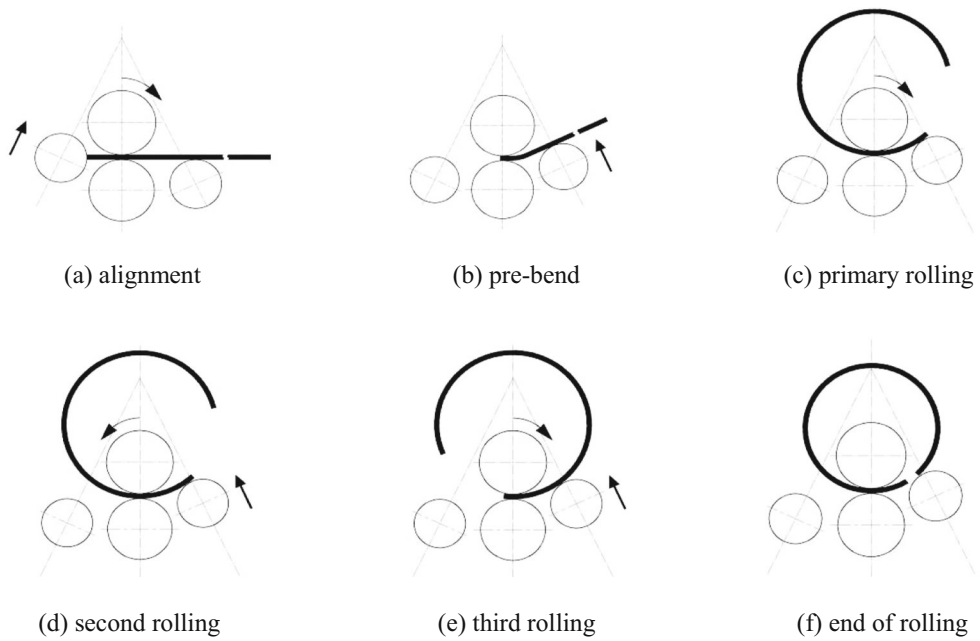

Fig. 1 Four-roll bending forming process

will not only reduce the number of subsequent roll bends and improve work efficiency, but also reduce the displacement of subsequent roll bends. In order to increase the displacement of the first rolling, the calculation accuracy of the roll bending forming model must be established. Taking into account that the plate bending forming is mainly elasto-plastic deformation, it is difficult to establish a high-accuracy rebound model. In engineering, based on the combination of theory and experience, the following plate springback model is generally used [12], as shown in Eq. (1):

$$R_a = \frac{1-K_0\sigma_s/E}{1+2R_fK_1\sigma_s/Et}R \tag{1}$$

In which R_a is the radius of sheet before rebound, R is the final radius of sheet, t is the thickness of the sheet, K_0 is the relative strengthening factor, K_1 is the shape factor, E is the Young's modulus, and σ_s is the material yield limit.

As shown in Fig. 2, it reflects the geometric relationship between the rolls. The mathematical relationship between the displacement of the side roll and the final forming radius of the plate established by the four-roll bending process model is shown in Eq. (2) [13].

$$f = L_2\left[\frac{\sin(\lambda-\beta+\varphi)\times\dfrac{\sin\varphi\times(R+t+R_3)}{\sin(\lambda-\beta)}}{\sin\varphi}\right]\Bigg/\left[\frac{\sin\beta\times\left(\dfrac{\sin\varphi\times(R+t+R_3)}{\sin(\lambda-\beta)}+R-R_1\right)}{\sin\lambda}\right] \tag{2}$$

where

R $\left(\frac{1-\frac{k_0\sigma_s}{E}}{1+\frac{2k_0\sigma_sR_a}{Et}}\right)R_a$

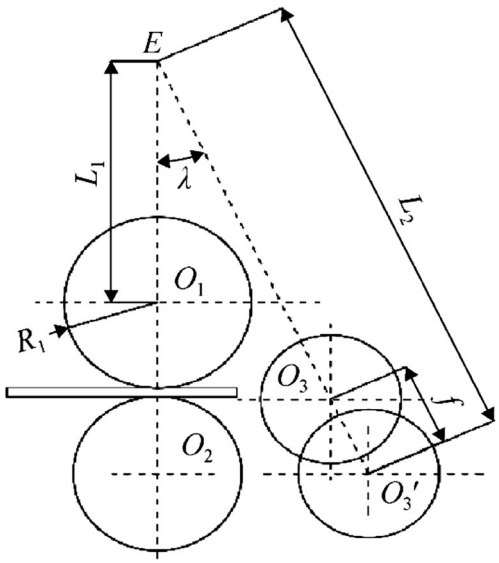

Fig. 2 Roll bending position

β $\arctan\left[\frac{B}{\sqrt{(R_a+t+R_2)^2-B^2}-(R_a-R_1)}\right]$

φ $\arcsin\left[\frac{L_1\sin\lambda-(R_a-R_1)\sin(\lambda-\beta)}{R_a+t+R_2}\right]$

B $2t$

In which f is the displacement of side roll, L_2 is the distance between the center of side roll and intersection point of the roll angle and center line in the initial state, R_1 is the diameter of top roll, R_2 is the diameter of bottom roll, and R_3 is the diameter of side roll.

In order to simplify the formula (2), Eq. (3) is established by power function to curve the relationship between the displacement of side roll and final forming radius of the sheet.

$$R = a\times^f b \tag{3}$$

In which $a = 2.817\text{e}+16$, $b = -4.696$.

As shown in Fig. 3, it reflects the relationship between displacement of the side roll and the radius of not rebound model, the radius of rebound model, relative bending curvature (ratio of sheet thickness to forming radius $\tilde{\kappa} = t/R$) and rebound ratio (ration of rebound forming radius to not rebound forming radius R/R_a). It can be seen from Fig. 3 that both the curve A and the curve B have relatively small deviation in the range of $R = 2\sim3$m. At this time, the relative bending curvature curve C of the plate is approximately proportionally monotonically increasing, and the rebound ratio curve D is approximately exponentially decreasing. This is because in the initial stage, the displacement of the side roll is small, and the plate mainly undergoes elastic deformation with its relative bending curvature $\tilde{\kappa}\leq0.025$, so the rebound of the plate is large after unloading. With the increase of the displacement of the side roll, its relative bending curvature $\tilde{\kappa} > 0$

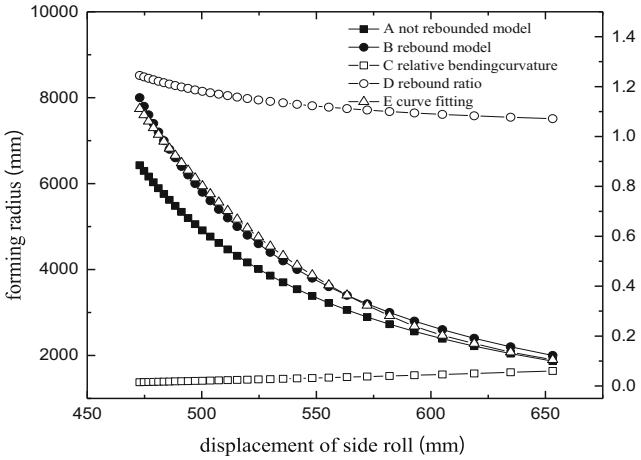

Fig. 3 Displacement of side roll-forming radius, relative bending curvature, and rebound ratio

.025 and the plate deformation gradually transitions to elasto-plasticity which lead to small rebound after unloading.

2.3 Multi-pass roll forming control algorithm

The forming radius of plate in the process of four-roll bending is affected by many factors, so there will be some deviation between the calculation results of the four-roll bending forming process model established in this paper and the experiment data; it is difficult to be directly used to solve multi-pass bending process parameters. The multi-pass roll bending process parameters must be determined by collecting actual roll bending data to improve the calculation accuracy of the theoretical model. Considering that the theoretical calculation is smaller than the actual data during roll bending process, in order to avoid the failure of forming radius, the displacement of side roll during the first pass bending cannot be too large. Therefore, when calculating the operating parameters of the four-roll bending machine, the displacement of the side roll during first pass bending can be determined according to formula (2). Trying to increase the amount of side roll displacement in the second and subsequent roll forming can reduce the number of roll bending and improve the forming efficiency.

In the roll forming process, the forming curvature of the plate after the first pass bending is close to the radius of the closed tube section, so the range of subsequent side roll movement is relatively small. When the roll radius R changes in a small range, the displacement of side roll and forming radius of sheet are approximately proportionally decreasing. In the case of multi-pass roll forming with plate thickness 120 mm and width 3500 mm, the forming radius of the plate $R_1 \approx$ 2726mm after first pass, and the forming radius of the closed plate $R_F \approx 2988$mm. The relationship between the amount of side roll movement and the final forming radius in the range of $R = 2.7$~3.0m is shown in Fig. 4. It can be seen that when the amount of side roll movement is small, the forming radius of the plate is approximately proportional to the displacement of side roll and the slope is abf^{b-1}.

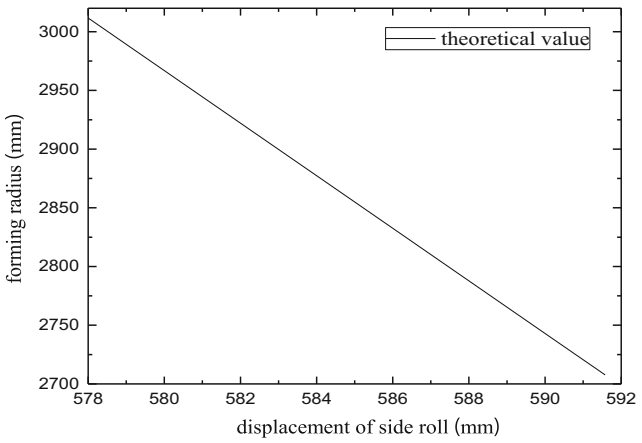

Fig. 4 Displacement of side roll-forming radius

The parameters d_{iSj}, d_{iEj}, and R_{ij} indicate the displacement of side roll and forming radius of the plate with the same specification at different times of different passes in multi-roll bending process. The subscript i indicates that the same type of plate is rolling for the i pass, and the subscript j indicates the number of passes. The subscript S indicates the initial of roll bending and the subscript E indicates the end of roll bending. The multi-pass roll-bending control algorithm of four-roll bending machine is as follows:

(1) When the plate is rolled for the first time, determine the displacement of side roll at the first pass according to formula (2), denoted as d_{1S1}; the final forming radius at the end of first pass is recorded as R_{11}; reverse rotation and move up side roll after forming, under the condition that the curvature radius of the plate does not increase, the maximum displacement value of the side roll is recorded as d_{1E1}; the arc plate becomes a closed tube section after many times of subsequent bending, record the amount of side roll displacement d_F and final forming radius R_F.

(2) When the same type of sheet is rolled again, the displacement d_{2S1} of the first side roll increases 1~2mm on the basis of d_{1S1}, and the forming radius in the end of first pass is recorded as R_{12}; obtained d_{2E1} using the method identified d_{1E1} in step (1); calculate the displacement and forming radius of second pass according to formula (4); after a number of simulation analysis, the side roll movement can be solved according to $K_2 = 2/3$; K is the displacement coefficient.

$$\begin{cases} d_{2S2} = k_2(d_F - d_{2E1}) + d_{2E1} \\ R_{22} = (1-k_2)(R_{21} - R_F) + R_F \end{cases} \tag{4}$$

(3) After the second pass bending process, record forming radius R_{22} and the displacement of side roll d_{2E2} at this time, according to formula (5) to calculate the displacement d_3 of third pass, it can be solved by $k_3 = 1/2$.

$$\begin{cases} d_{iSj} = k_j\left(d_F - d_{iE(j-1)}\right) + d_{iE(j-1)} \\ R_{ij} = \left(1-k_j\right)\left(R_{i(j-1)} - R_F\right) + R_F \end{cases} \quad (i = 2, 3\ldots; j = 3, 4\ldots) \tag{5}$$

(4) Repeat step (3), gradually adjust k_i until plate becomes closed cylinder.

(5) When rolling the same plate for the third time, gradually improve k_i in steps (3) and (4).

3 Finite element model of four-roll bending process

3.1 Model problem

Because very small time increments were needed in the problem, it has been confirmed by Han et al. [14] that the explicit solution method seemed more suitable compared with implicit method. Due to the small deformation of the roller during roll bending, it can be set as a rigid body; a steel sheet was assigned as a deformable body. According to the actual parameters of the W160 × 3500 four-roll coiler (top roll diameter is 1200 mm, bottom roll diameter is 1100 mm, side roll diameter is 900 mm, roll angle is 25°), the finite element model was defined as shown in Fig. 5. The thickness of the plate is 120 mm; selecting the deformable plane strain element, cell type is 4-node linear reduction integration unit CPS4R.

3.2 Material model

Q235B steel plate is used in the simulation; material properties are as follows: yield stress is 235 MPa, Young's modulus is 210 GPa, Poisson's ratio is 0.3, density is 7800 kg/m^3, and strengthen coefficient is 1900. It is assumed that the sheet material is isotropic and the weight of the sheet is not considered. Table 1 shows the properties of the Q235B sheet.

The bilinear model was used to describe the constitutive relationship of the sheet to simulate the plastic deformation during roll forming. The constitutive equation is shown in Eq. (6):

$$\sigma = \begin{cases} E\varepsilon & 0 < |\varepsilon| < \varepsilon_e \\ \sigma_s + K(\varepsilon - \varepsilon_e) & \varepsilon_e < |\varepsilon| \end{cases} \tag{6}$$

In which σ for stress (MPa), σ_s for yield limit (MPa), ε for strain, ε_ε for elastic strain limit, and K for strengthen coefficient.

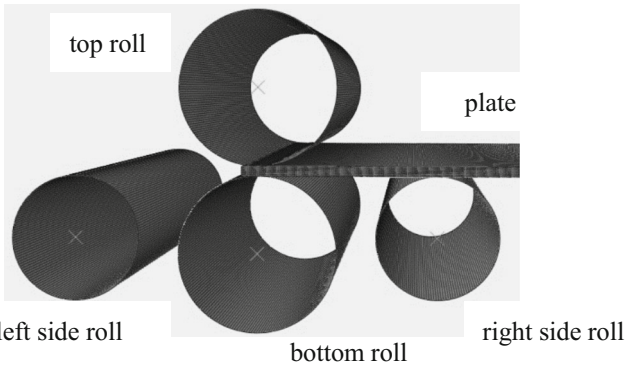

Fig. 5 Diagram for the finite element model of four-roll bending

3.3 Contact definition

The contact property between different parts of a rolling machine can be defined as surface to surface contact [15]; a master–slave contact approach is used in an analysis where the rollers are considered as the master surfaces, and the sheet surfaces facing the rollers constitute the slaves. The Coulomb friction law is used for the contact surfaces; in order to reduce the resistance of the right roll to the plate and ensure continuous and stable feeding of sheet during roll bending, all friction coefficients were also assumed to be constant during the rolling process. Tailor et al. [16] pointed out that friction has a great influence on plastic forming results. Therefore, in order to improve the accuracy of the simulation model, it is necessary to select the appropriate friction coefficient. McConnell et al. [17] believe that the friction coefficient has a correspondence relation with roll force, roll torque, and forward slip, so the coefficient of friction is determined according to different lubrication conditions. In the case of better lubrication, the friction coefficient calculated by the Hill's formula is adequate. Therefore, the rolling friction coefficient is 0.1, which is in line with the actual situation. The interaction between the plate and rollers was formulated using the finite sliding approach, which allowed the possibility of separating the surfaces during the rolling operation.

4 Simulation analysis of multi-pass

4.1 Analysis of stress and strain of multi-pass

The distribution of equivalent stress in the roll bending deformation zone affects the final forming quality of the plate. By comparing the stress and strain fields in the deformation zone under different roll-bending times, the effect between the number of roll-bending and forming quality is analyzed. When the displacement of side roll is 580 mm, the stress distribution in the roll-bending deformation zone is shown in Fig. 6.

Due to work hardening caused by the roll bending process, the yield strength of the plate material is increased, so the bending moment applied during the next roll

Table 1 The specifications and material properties of Q235B sheet

Thickness T (mm)	Width W (mm)	Young's modulus E (GPa)	Yield stress σ_s (MPa)	Strengthen coefficient K	Density ρ (kg/m^3)
120	2500	210	235	1900	7800

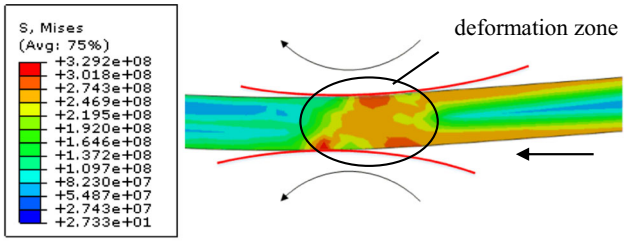

(a) Equivalent Mises stress of the first pass

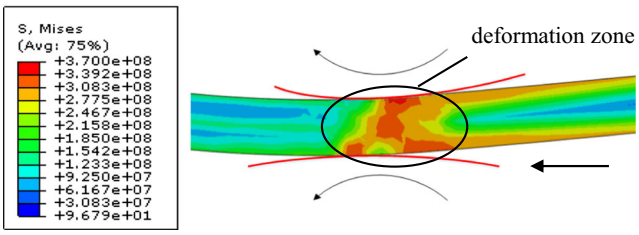

(b) Equivalent Mises stress of the third pass

Fig. 6 Equivalent stress comparison between first pass and third pass. **a** Equivalent Mises stress of the first. **b** Equivalent Mises stress of the third

bending must be increased. It can be seen from Fig. 6 that the equivalent stress value in the three-pass continuous roll bending is higher than that in the firs-pass roll bending, and the extremum value rises from 329.2 to 370 MPa.

Further comparative analysis of the equivalent plastic strain distribution in the deformation zone is shown in Fig. 7. It can be found that the plastic strain distribution of multi-pass on the cylinder surface is more uniform than that of first pass. The plastic strain fluctuations on the cylinder surface with multi-pass process are significantly reduced. The plastic strain fluctuation decreased from 0.004 at first pass to 0.001 at fifth pass and the consistency of forming radius was significantly improved. Therefore, the multi-pass roll bending can effectively improve the forming quality.

Figure 8 shows the distribution of equivalent stress in the thickness direction from the inner surface node 1 to the outer surface node 7 during single-pass, three-passes, and five-passes roll bending. It can be seen that the distribution of the equivalent stress field in the deformation zone is symmetrical with respect to the neutral layer, irrelevant to the number of passes, and the maximum stress is at the inner and outer surfaces of the plate. Because work hardening caused by multi-pass bending will increase the yield strength of the material, the stress values on the upper and lower surfaces of the plate will increase with the number of roll bending. The elastic deformation occurs near the plate neutral layer, so the equivalent stress will remain basically unchanged and has nothing to do with the number of passes.

4.2 Forming by three pass

In order to improve work efficiency during roll bending, it is necessary to use as few passes as possible to achieve the required machining accuracy. In order to explore the feasibility of three pass roll forming, three multi-passes processes are designed for large-size thick-walled tube sections, as shown in Table 2.

According to the multi-pass roll forming control algorithm, the multi-passes roll forming process scheme in Table 2 was established for the finite element simulation test. As shown in Fig. 9, it reflects the relationship between the forming radius and displacement of side roll by five passes roll bending control algorithm. From the comparison results, it can be seen that there is small deviation between theoretical value and simulation test value in the first and second pass, while the difference between the theoretical value and the simulation test value in third pass is larger; this is due to excessive displacement of side roll. The larger side roll movement in the third pass helps to reduce the deviation between the theoretical value and simulation test value in subsequent pass. The error in the fourth pass and the fifth pass decreases significantly, at the same time, the third to fifth pass of the simulation test have very little difference in radius, which helps to improve the accuracy of the roll curvature distribution. Because of the small movement of side roll in fifth pass ($f = 3$ mm), it did not cause the tube to be deformed, so the simulation radius of the fourth and fifth roll bending was basically the same.

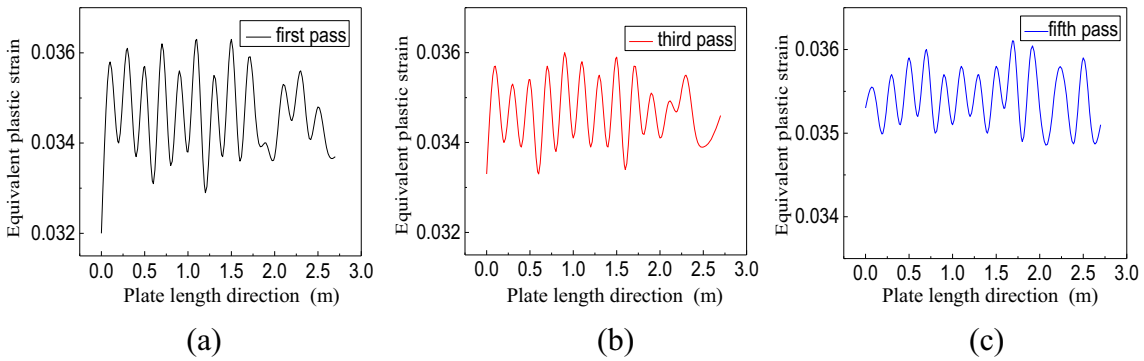

Fig. 7 Fluctuation of equivalent plastic strain in multi-pass roll bending process

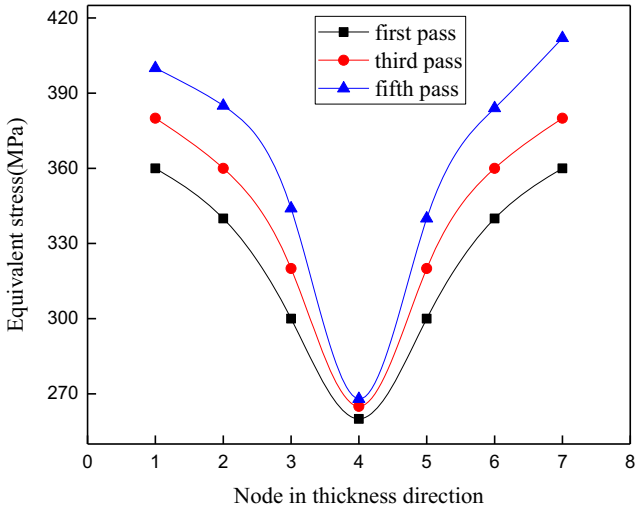

Fig. 8 Distribution of equivalent stress along thickness direction

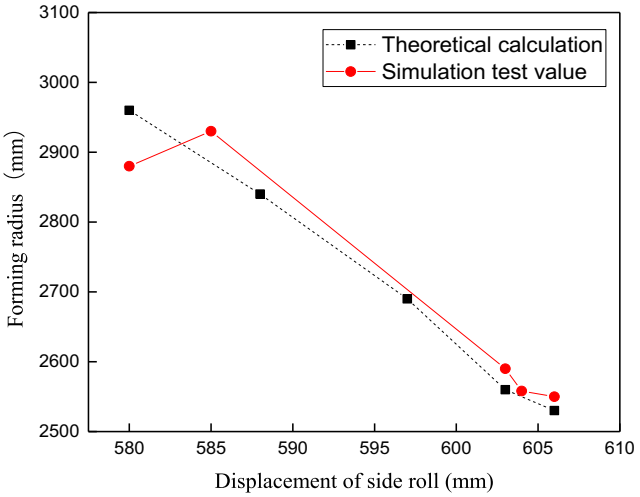

Fig. 9 Theoretical and simulation curves of side roll movement in four-pass bending process

Figure 10 reflects the relationship between the forming radius and displacement of side roll by four passes roll bending control algorithm. It can be seen that there is small deviation between theoretical value and simulation test value in the first and second pass, while the difference is large in third pass. It ensures theoretical value and simulation test value are in good agreement in fourth pass, which helps improve the forming accuracy.

By gradually adjusting the parameters of the four-passes bending process, the sheet can be rolled into a closed tube section during the third pass that means the realization of three-passes bending forming. Figure 11 shows the relationship between the forming radius and displacement of side roll by four passes roll bending control algorithm.

From formula (2), it can be seen that the plate thickness has little effect on the relationship between displacement of side roll and the forming radius. Therefore, the multi-pass roll forming control algorithm has wide adaptability.

Combining the above multi-pass roll bending data, the following conclusions can be drawn: The displacement of side roll in the first pass is particularly critical during forming the large tube section, formula (2) is used to calculate the displacement of side roll in the first pass, and adjusting the displacement of side roll calculated in previous roll bending test can achieve four-pass forming in second roll bending test. In the subsequent roll bending test, when the forming radius in the first pass is less than the secondary forming radius in four-pass roll bending scheme, three-pass bending forming is achieved.

Table 2 Multi-pass roll forming process scheme

Sheet thickness	No.	Rolling scheme
Sheet *I*: $t = 120$mm	1	Five pass ($k_2 = 1/3$, $k_3 = 1/2$, $k_4 = 2/3$, $k_5 = 1$)
	2	Four pass ($k_2 = 1/3$, $k_3 = 1/2$, $k_4 = 1$)
	3	Three pass ($k_2 = 1/3$, $k_3 = 1$)

5 Verification of multi-pass roll forming control algorithm

The coiled tube section has welding steps in the subsequent operation. The uniform distribution of forming radius in circumferential direction can effectively reduce subsequent operations and improve processing efficiency. In order to verify the applicability and accuracy of the multi-pass roll forming control algorithm, analyzing the effect of the roll bending number, the displacement of side

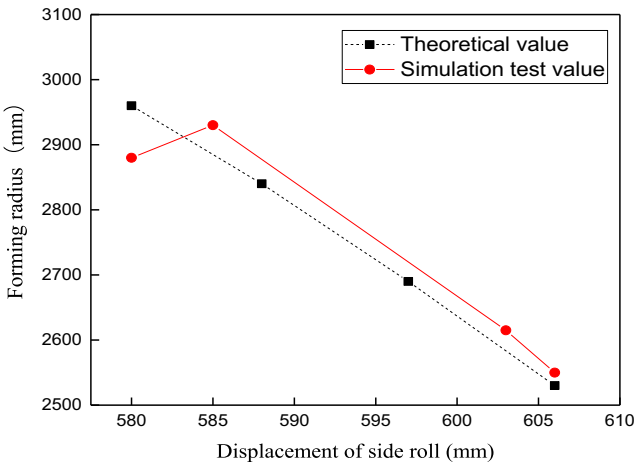

Fig. 10 Theoretical and simulation curves of side roll movement in four-pass bending process

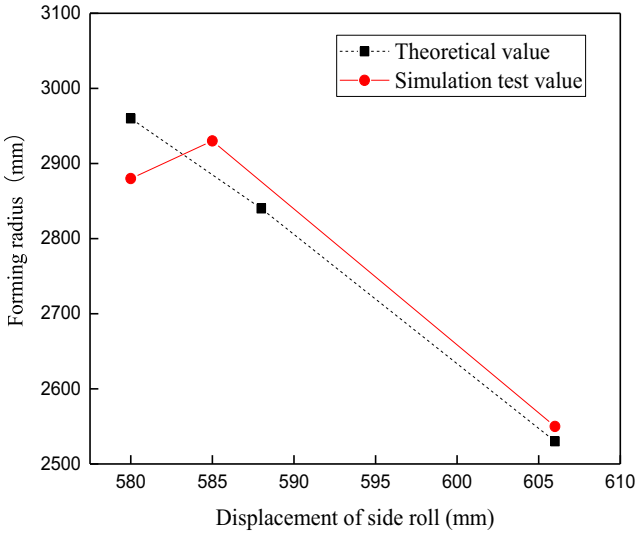

Fig. 11 Theoretical and simulation curves of side roll movement in three-pass bending process

roll on the first pass, and the distance between the side roll in subsequent pass on the forming quality and efficiency during multi-pass bending forming process, multi-pass four-roll bending forming simulation experiment was performed on Q235B steel plate.

According to the five-pass bending forming comparison test scheme shown in Table 3, the displacement of side roll was adjusted. The displacement of side roll in test 1 was calculated according to multi-pass roll forming control algorithm ($f_2 = 8$, $f_3 = 9$, $f_4 = 6$, $f_5 = 3$); the interval difference of side roll movement in test 2 was the same ($f = 10$); the displacement of side roll in test 3 is taken random ($f_2 = 10$, $f_3 = 10$, $f_4 = 3$, $f_5 = 3$).

According to the four-pass bending forming comparison test scheme shown in Table 4, the displacement of side roll was adjusted. The displacement of side roll in test 4 was calculated according to multi-pass roll forming control algorithm ($f_2 = 8$, $f_3 = 9$, $f_4 = 9$); the interval difference of side roll movement in test 5 was the same ($f = 8.6$); the displacement of side roll in test 6 is taken randomly ($f_2 = 10$, $f_3 = 10$, $f_4 = 6$).

According to the three-pass bending forming comparison test scheme shown in Table 5, the displacement of side roll was adjusted. The displacement of side roll in test 7 was calculated according to multi-pass roll forming control algorithm ($f_2 = 8$, $f_3 = 18$); the interval difference of side roll movement in test 8 was the same ($f = 13$); the displacement of side roll in test 9 is taken in random ($f_2 = 10$, $f_3 = 16$).

Table 4 Comparison of the test scheme of four-pass bending forming

No.	First pass	Second pass	Third pass	Fourth pass
4	580 mm	588 mm	597 mm	606 mm
5	580 mm	588.6 mm	597.2 mm	606 mm
6	580 mm	590 mm	600 mm	606 mm

After the multi-pass roll bending test is completed, the formed tube is divided into five segments in the circumferential direction, and a digital radius measuring instrument is used to measure the inner diameter value of the middle section in every segmented section. As shown in Fig. 12, it reflects the distribution of the forming radius under different multi-pass roll bending test scheme.

As can be seen in Fig. 12, using the scheme of tests 1, 4, and 7 carried out by multi-pass roll forming control algorithm, the forming radius distribution is relatively uniform, and the calculated mean square deviations of forming radius are 10.1 mm, 12.3 mm, and 18.6 mm, respectively; when the multi-pass roll bending was carried out using the scheme of tests 2, 5, and 8, the mean squared deviations of forming radius are 13.6 mm, 14.2 mm, and 23.1 mm, respectively; when using the scheme of tests 3, 6, and 9 to perform multi-pass roll bending, the mean square deviations of forming radius are 15.1 mm, 15.2 mm, and 22.1 mm, respectively. The test results show that the multi-pass roll forming control algorithm can effectively improve the forming quality of the plate with the same rolling passes.

With the increasing of rolling passes, the forming radius of the plate has also increased from 2134 to 2450 mm, which is mainly due to the work hardening during the multi-roll bending. The greater the number of rolling passes, the greater the yield strength of the surface and the greater the resistance to deformation, resulting in plastic deformation area increase, a decrease in the spring back, and an increase in the forming radius of the sheet.

Table 3 Comparison of the test scheme of five-pass bending forming

No.	First pass	Second pass	Third pass	Fourth pass	Fifth pass
1	580 mm	588 mm	597 mm	603 mm	606 mm
2	580 mm	586.5 mm	593 mm	599.5 mm	606 mm
3	580 mm	590 mm	600 mm	603 mm	606 mm

Table 5 Comparison of the test scheme of three-pass bending forming

No.	First pass	Second pass	Third pass
7	580 mm	588 mm	606 mm
8	580 mm	593 mm	606 mm
9	580 mm	590 mm	606 mm

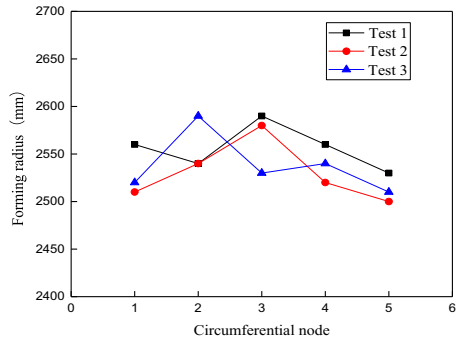

(a) Forming radius distribution of circumferential direction in five-pass roll bending

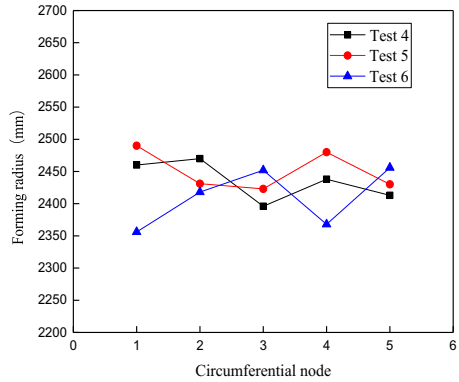

(b) Forming radius distribution of circumferential direction in four-pass roll bending

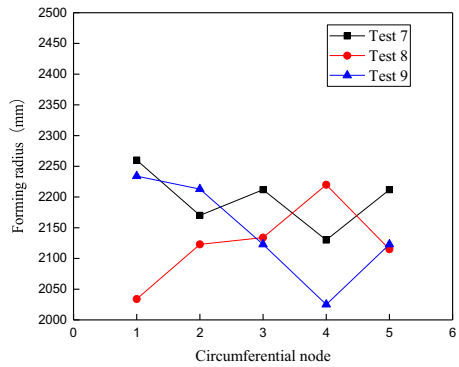

(c) Forming radius distribution of circumferential direction in three-pass roll bending

Fig. 12 Forming radius distribution of circumferential direction in multi-pass roll bending. **a** Forming radius distribution of circumferential direction in five-pass roll bending. **b** Forming radius distribution of circumferential direction in four-pass roll bending. **c** Forming radius distribution of circumferential direction in three-pass roll bending

6 Conclusion

Dynamic analysis with a four-roller machine was performed using the Abaqus/Explicit code. First, a four-roll bending forming process model was established to obtain required forming radius by moving side roll. Finite element model was then developed to analyze the difference between different rolling passes. Finally, in order to reduce the number of roll bends and improve the forming accuracy, the multi-pass roll forming control algorithm was set up, and it was validated by comparing the theoretical and experimental results. The result shows that the multi-pass roll forming control algorithm can increase the uniformity of the forming radius and reduce the variance of the curvature when the number of roll bends is the same. When the algorithm is used to solve operation parameter, if using five-pass roll forming, the calculation can be performed with $k_2 = 1/3$, $k_3 = 1/2$, $k_4 = 2/3$, $k_5 = 1$; if using four-pass roll forming, the calculation can be performed with $k_2 = 1/3$, $k_3 = 1/2$, $k_4 = 1$; for three-pass roll forming, $k_2 = 1/3$, $k_3 = 1$ can be used for calculation.

References

1. Milenin AA, Dyja H, Mróz S (2004) Simulation of metal forming during multi-pass rolling of shape bars. J Mater Process Technol 153–154(1):108–114
2. Chen Z, Wang D, Cao X, Yang W, Wang W (2018) Influence of multi-pass rolling and subsequent annealing on the interface microstructure and mechanical properties of the explosive welding Mg/Al composite plates. Mater Sci Eng A 723:97–108
3. Gandhi AH, Shaikh AA, Raval HK (2009) Formulation of springback and machine setting parameters for multi-pass three-roll cone frustum bending with change of flexural modulus. Int J Mater Form 2:45–57
4. Luksza J, Burdek M (2002) The influence of the deformation mode on the final mechanical properties of products in multi-pass drawing and flat rolling. J Mater Process Technol 125-126:725–730
5. Hua M, Sansome DH, Baines K (1995) Mathematical modeling of the internal bending moment at the top roll contact in multi-pass four-roll thin-plate bending. J Mater Process Technol 52(2):425–459
6. Yu G, Zhao J, Zhai R, Ma R (2018) Theoretical analysis and experimental investigations on the symmetrical three-roller setting round process. Int J Adv Manuf Technol 94:45–46
7. Fu Z, Tian X, Chen W, Hu B (2013) Analytical modeling and numerical simulation for three-roll bending forming of sheet metal. Int J Adv Manuf Technol 69:1639–1647
8. Ktari A, Antar Z, Haddar N, Elleuch K (2012) Modeling and computation of the three-roll bending process of steel sheet. J Mech Sci Technol 26(1):123–128
9. Shivpuri R, Shin W (1992) A methodology for roll pass optimization for multi-pass shape rolling. Int J Mach Tool Manu 32(5):671–683
10. Yuan SY, Zhang LW, Liao SL, Jiang GD, Yu YS, Qi M (2009) Simulation of deformation and temperature in multi-pass continuous rolling by three-dimensional FEM. J Mater Process Technol 209(6):2760–2766
11. Shin W, Lee SM, Shivpuri R, Altan T (1992) Finite-slab element investigation of square-to-round multi-pass shape rolling. J Mater Process Technol 33(1):141–154

12. Li S, Chen F, Li b (2011) Calculation of side roll displacement for four-roll bending plate process. Forging & Stamping Technol 36(6): 76–79
13. Wang Y, Zhu X, Hu J, Cui X (2018) Research on numerical simulation of continuous roll forming process of four-roll plate bending machines. Journal of System Simulation 30(5):1772–1780
14. Han X, Hua L (2009) 3D FE modeling of cold rotary forging of a ring workpiece. J Mater Process Technol 209(12):5353–5362
15. Ktari A, Antar Z, Haddar N, Elleuch K (2012) Modeling and computation of the three-roller bending process of steel sheets. J Mech Sci Technol 26(1):123–128
16. Tailor VK, Gandhi AH, Moliya RD, Raval HK (2008) Finite element analysis of deformed geometry in three-roller plate bending process. MSEC 1:609–616
17. McConnell C, Lenard JG (2000) Friction in cold rolling of a low carbon steel with lubricants. J Mater Process Technol 99(1):86–93